Automatic Three-Dimensional Point Cloud Processing for Forest Inventory

Jean-François Lalonde, Nicolas Vandapel and Martial Hebert

CMU-RI-TR-06-21

The Robotics Institute
Carnegie Mellon University
5000 Forbes Avenue
Pittsburgh, Pennsylvania 15213, USA

Abstract

In this paper, we propose an approach that enables automatic, fast and accurate tree trunks segmentation from three-dimensional (3-D) laser data. Results have been demonstrated in real-time on-board a ground mobile robot. In addition, we propose an approach to estimate tree diameter at breast height (dbh) that was tested off-line on a variety of ground laser scanner data. Results are also presented for detection of tree trunks in aerial laser data. The underlying techniques using in all cases rely on 3-D geometry analysis of point clouds and geometric primitives fitting.

Contents

1 Introduction

Developing techniques for accurate, exhaustive and cost-effective forest inventory is a challenging but necessary task that allows a better management of extensive natural resources. Forest inventory encompasses numerous types of measurements, done at different spatial scale and repeated over time, as detailed in [16]. This paper deals with the basic, but fundamental, task of counting trees and estimating their trunk diameter.

Traditionally labor intensive, forest inventory has seen a dramatic shift with the introduction of aerial imagery that can be used for counting trees, determining species and potentially their height. With such techniques, large areas can be automatically processed. Large- and small-footprint aerial laser scanners can address some of the limitations from overhead imagery, specifically the recovery of the tree canopy three-dimensional (3-D) structure. The development of ground laser scanners has provided new tools to collect better (in terms of accuracy and point density) 3-D information from forest, but the huge amount of data to process requires reliable automatic data processing techniques. In addition, the variety of information sources available, both from the ground and the air, requires the development of generic techniques for automatic 3-D point cloud processing. This paper presents a framework to address those issues.

In the context of ground mobile robotics in natural environments, we developed algorithms to automatically process 3-D data in order to estimate the ability of a robot to traverse the perceived terrain. Those obstacle detection and scene interpretation tasks led us to implement generic techniques for the classification, segmentation, interpretation, and modeling of 3-D point clouds [8]. Unlike traditional methods used in robotics, we work only in the three-dimensional space along the data processing pipeline. The capabilities of such techniques have been demonstrated in real-time on-board a mobile robot. They also have been demonstrated over a variety of terrains and sensors. In this paper, we present how such method can be used in the context of forest inventory for automatically segmenting tree trunks and recovering their diameter at breast height. Figure 1 presents the automatic segmentation and interpretation of a scene scanned from the ground.

This paper is divided into five sections. Section 2 presents relevant references on sensors used to collect data and techniques to interpret those data for forest inventory. Section 3 contains an overview of the approach used for generic scene interpretation with an emphasis on geometric fitting. A set of results from various ground laser scanner and overhead data is presented in Section 4. We discuss in Section 5 the benefit of our approach for practical and cost effective forest inventory.

2 State of the art

This section focuses on ground-based methods for forest inventory, specifically on the sensor technology used, the fitting techniques employed, and the information recovered.

Terrestrial scanners have been used extensively in civil engineering and architecture to scan buildings, dams, bridges and statues. These applications focus on piece-wise

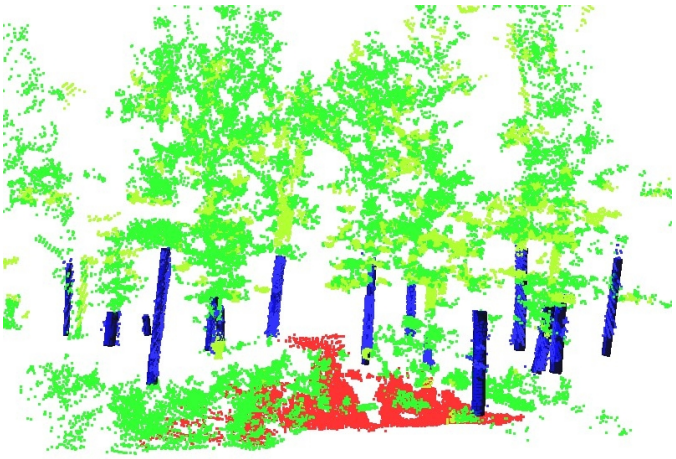

Figure 1: Example of automatic tree trunks segmentation. In red, the ground surface; in green/yellow the foliage/grass and linear structures; in blue, fitted cylinders to the segmented tree trunks.

continuous surfaces, very much different from vegetated terrain with porous medium and linear structures. Several authors initiated work on evaluating the performances of such scanner for forest inventory, see for example [15]. Unfortunately, such high-resolution, high-density scanners are expensive, slow and not well suited for field deployment. Some laser scanners with similar performances are designed explicitly for forestry [5]. In both cases, they generate a huge amount of data, up to several millions points per scan, that prevent in-the-field data processing. In this paper, we present results from several laser scanners but show how an actuated SICK laser scanner, rugged and affordable, is suitable for forestry.

Single point laser scanners have also been used in combination with a camera to extract measurements from tree trunks [2]. By mosaicking the images, a complete 2D-1/2 texture model of a can be produced as proposed in [4]. Both cases require the aiming of the laser at the area of interest. Another work by [7], does not use any laser range finder but instead proposes to use a calibrated camera in conjunction with a know geometric target. This approach is not effective as it requires the positioning of the target along the tree to measure. Image-based systems face the challenging problem of segmenting tree trunks or branches from cluttered background scene.

For closer range applications, [6] developed an approach based on a laser line striper. Such hand-held instruments require extensive human intervention to aim them at selected targets. With our proposed approach, large point clouds can be processed and multiple trees can be recovered.

Several authors proposed methods to fit cylinders or active contours to tree trunks or branches to model them [12] [13]. Such approach assumes implicitly that the tree is isolated and not cluttered by foliage or ground vegetation. In addition, some requires the accumulation of data from multiple viewpoints and the use of high density laser scanner. In this paper, we present an approach to automatically detect tree trunks, seg-

ment them and recover their diameters, without any assumptions on the environment. Our approach is not as accurate as [13] for example, because we neglect the ovality of the tree stems that cannot be captured by cylinder fitting.

In addition to extracting geometric information about trees as presented in the previous paragraph, forest inventory also encompasses the estimation of wood quality. Schutt [14] investigates the use of reflectance information in high resolution, high density laser data to detect wood defects. This task is not considered in this paper, as our approach relies only on geometric information that cannot capture such defects.

3 Technical approach

The proposed approach relies on four steps: point-wise classification, segmentation, interpretation, and high-level scene modeling. This section is an overview of the approach tested on-board an autonomous mobile robot. Additional details can be found in [8] and [17].

3.1 Point cloud classification

The first step of the process consists in the classification of a 3-D point cloud into three classes: linear structures (corresponding to branches or thin tree trunks), solid surfaces (corresponding to large tree trunks or ground surface) and scattered points (corresponding to ground vegetation, foliage and tree canopy). This step relies on the 3-D geometric analysis of local point distribution through the use of the scatter matrix. The features distributions for the three basic classes are learned off-line from labeled data. Finally, Bayesian classification is performed on-line.

3.1.1 Features extraction

Let $N(X,R) = \{Y \in \Re^3 \mid \|X - Y\| \leq R\}$ be the set of points Y that fall in the local 3-D region, centered at X, that needs to be characterized. The scatter matrix S is computes as

$$S = \frac{1}{card(N)} \sum_{Y \in N(X,R)} (Y - \overline{Y})(Y - \overline{Y})^T$$

using the points from that area and extract the principal components. Let's call $\lambda_2 \leq \lambda_1 \leq \lambda_0$ the ordered eigenvalues and the corresponding eigenvectors. The point cloud can be classified as:

- Random. There is no principal direction and $\lambda_0 \simeq \lambda_1 \simeq \lambda_2$, we choose scatterness = λ_0 as feature.

- Linear. There is one large and two small eigenvalues: $\lambda_2 \simeq \lambda_1 \ll \lambda_0$. The feature is chosen as linear-ness = $(\lambda_0 - \lambda_1)e_0$, aligned with the local tangent to the point cloud structure.

- Surface. There are two large eigenvalues and one small: $\lambda_2 \ll \lambda_1 \simeq \lambda_0$. The feature is chosen as surface-ness = $(\lambda_1 - \lambda_2)e_2$, aligned with the local normal.

3.1.2 Features distribution modeling

We fit a Mixture of Gaussians to the features distribution using the Expectation Maximization algorithm [1]. We impose the number of Gaussians per class, typically three, and recover automatically the centroid, principal axes and associated covariances.

3.1.3 On-line classification

Maximum likelihood classification is used to recover the class and normalized confidence in classification. This procedure is sensor-independent and parameter-free as machine learning techniques are used to capture automatically the point cloud distribution from training data for each class. Figure 7 presents such an example for a forest scene with large trees. Individual 3-D points are classified into surface (red), linear (blue) or vegetation (green).

3.2 Point cloud segmentation

The second step consists of the extraction of connected components that groups together the individual 3-D points based on their class and the local consistency of the direction of the features, either the local tangent or local normal, within some support region.

3.3 Interpretation

Context-based knowledge is used to semantically interpret the data based on the direction, size, smoothness and continuity of each component. In addition, the spatial and classification relationship between components is also taken into account. We can isolate tree trunks the following way. First, the ground is defined as being the largest surface with the lowest elevation. The ground is then meshed and stored as a digital elevation map. To identify tree trunks from all the other linear structures extracted (ex: branches), the distance between the object and the closest point on the ground is computed, and the structure is identified as a trunk if the distance lies below a certain threshold. Moreover, the angle with the vertical direction is also evaluated. Our method is robust to these parameters: they were chosen based on experimentation and are kept constant through all the results shown in Section 4.

3.4 High-level scene modeling

The final step consists in high-level scene modeling by fitting geometric primitives to the different components extracted, allowing a compact and accurate representation of the environment that preserves the geometric and semantic properties of the scene. Different level of details can be achieved depending on the application considered (mobility analysis versus forestry).

Once the 3-D points are grouped, cylinders are fitted onto each of the components representing tree trunks. For each tree, its diameter should correspond to the extracted cylinder diameter. In this work, two different cylinder fitting techniques have been implemented: 2-D projection detailed in Section 3.4.1 and 3-D fitting presented in Section 3.4.2. Note that, in this section, new notations are introduced on purpose in order to distinguish the cylinder fitting presented here from the features extraction process (Section 3.1.1). Each component g_k has n 3-D points, noted $p_i = [x_i\ y_i\ z_i]^T$ for $i = 1...n$. Let μ be the center of mass

$$\mu = \frac{1}{n}\sum_{i=1}^{n} p_i \tag{1}$$

The k^{th} cylinder is parameterized by its radius r_k, its center c_k, its orientation o_k and its length l_k. Since each group is processed independently, the subscript k is dropped for clarity.

3.4.1 2-D projection

The goal of this technique is to provide a good approximation of the tree diameter while being very fast to compute. The idea is to project all the data points on a plane perpendicular to the principal direction, and fit a circle on that plane. Under the assumption that the local diameter and shape of a tree trunk stays constant, we expect this method to yield good results. First, the principal directions of the group g_k are found by computing the covariance matrix C of the points:

$$C = \frac{1}{n}\sum_{i=1}^{n}(p_i - \mu)(p_i - \mu)^T \tag{2}$$

and by extracting its eigenvalues and eigenvectors. If the eigenvalues are defined by $\lambda_0 \leq \lambda_1 \leq \lambda_2$, then the corresponding eigenvectors e_0 and e_1 define a plane Π, perpendicular to the main direction in the data (see Figure 3).

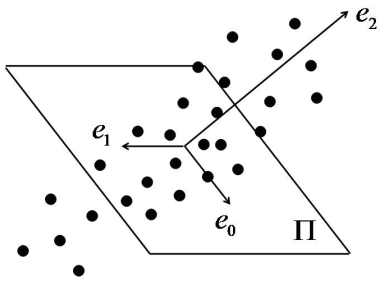

Figure 2: Axis and corresponding projection plane.

All the points p_i are then projected onto Π to yield the projected points q_i:

$$q_i = [e_0\ e_1]^T (p_i - \mu) \tag{3}$$

To speed-up processing and improve accuracy, only a subset $S_q = \{q_i \mid \tau_{min} < \|q_i\| < \tau_{max}\}$ of the q_i is used for fitting. The interval $[\tau_{min}, \tau_{max}]$ is taken such that it is centered at breast-height and is defined according to the expected number of points at a given distance. Its choice is data-driven, i.e. it depends on the environment and the sensor's characteristics. It is also application-oriented as it aims specifically at tree diameter estimation.

Finally, a 2-D circle is fitted onto the projected points $q_i \in S_q$ using Taubin's approximation [3], and its parameters (radius r_c and center c_c) are used to reconstruct the k^{th} cylinder in 3-D using equations (4)-(7):

$$r_k = r_c \tag{4}$$

$$o_k = e_2 \tag{5}$$

$$l_k = max_i(p_i^T o_k) - min_i(p_i^T o_k) \tag{6}$$

$$c_k = \mu_k + c_c(1)e_0 + c_c(2)e_1 \tag{7}$$

where $c_c(i)$ represents the i^{th} component of c_c, in the plane Π reference frame. Figure 3 shows an example of a fitted circle from real data. The recovered cylinder is shown in Figure 4. This process is very fast as the circle estimation is direct and does not require any iterative process, and is therefore suitable for real-time implementation.

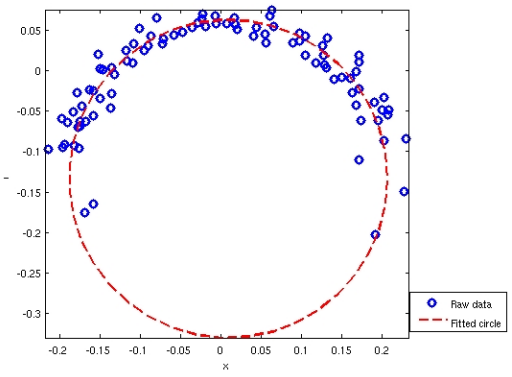

Figure 3: Circle fitted onto projection of 3-D points. The plane is centered on μ.

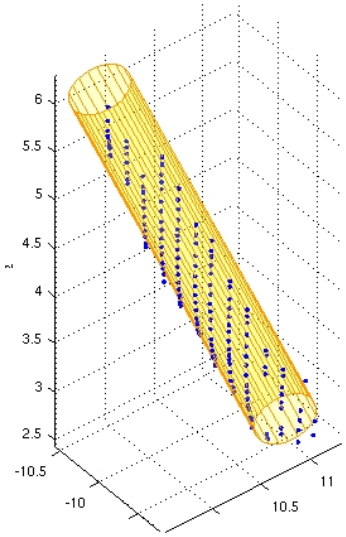

Figure 4: Cylinder fitting with 2-D projection results, blue points are 3-D points.

3.4.2 3-D fitting

In the hope of increasing diameter estimation accuracy, we compare with 3-D cylinder fitting. This process is iterative, and requires a larger amount of computations. The technique introduced by [10] is used and summarized here briefly. In the fitting process, we wish to minimize the following expression:

$$\sum_{i=1}^{n} d(s, p_i)^2 \tag{8}$$

where s is a set of parameters defining the cylinder, and $d(s, p_i)$ a distance function between a point p_i and the surface. Some constraints are defined on s. As proposed by [10], the approach reduces the problem to an unconstrained problem in a lower dimensional space by eliminating unknowns.

This is done using the following observation. If the distance function can be written as:

$$d(s, p_i) = \sqrt{g} - h \tag{9}$$

where g and h may be functions of s and p_i, then we can approximate d by

$$\tilde{d}(s, p_i) = \frac{g - h^2}{2h} \tag{10}$$

This simplification is much easier to compute, but still has the same zero set and derivatives at the zero set. Therefore, we can solve using Levenberg-Marquadt optimization. In the case of cylinders, we can parameterize the cylinder by $s = [k\ \rho\ a\ n]$ (see Figure 5) and the distance function can be expressed by

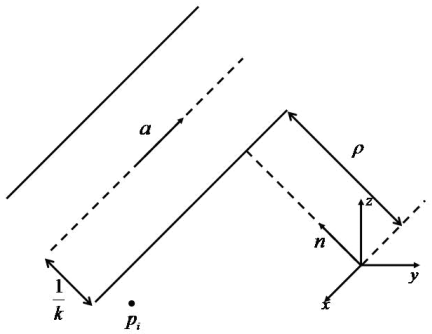

Figure 5: Parameterization used for cylinder fitting

$$d(s, p_i) = \|p_i - (\rho + \frac{1}{k}) \times a\| - \frac{1}{k} \quad (11)$$

$$= \sqrt{\langle p_i - (\rho + \frac{1}{k})n, p_i - (\rho + \frac{1}{k})n \rangle} - \frac{1}{k} \quad (12)$$

which has the form of Equation 9 with $<,>$ the dot product operator. We can therefore approximate Equation 12 with

$$\tilde{d}(s, p_i) = \frac{k}{2}\|\hat{p}_i \times a\|^2 - \langle \hat{p}_i, n \rangle \quad (13)$$

where $\hat{p}_i = p_i - \rho n$.

The optimization process finds the value of s_{opt} that minimizes this distance function, or the cylinder that best models the data. We use the parameters found by the 2-D projection technique presented earlier as a starting point for the optimization. The k^{th} cylinder parameters can be recovered from s_{opt}:

$$r_k = \frac{1}{k} \quad (14)$$

$$o_k = a \quad (15)$$

$$l_k = max_i(p_i^T o_k) - min_i(p_i^T o_k) \quad (16)$$

$$c_k = (min_i(p_i^T a) + \frac{l_k}{2})a + (\rho + \frac{1}{k})n \quad (17)$$

The 3-D fitting technique just described yields results approximately 25% worst than with the 2-D projection. The 3-D fitting is most likely sensitive to noise, that is better averaged by the 2-D projection, since the density of points on the circle is higher than the density on the cylinder.

4 Results

In this section, we present representative results of our current capabilities in term of data acquisition and real-time data processing processing, versatility of the approach, and precision in diameter estimation.

4.1 Real-time data processing on-board a ground mobile robot for mobility analysis

Figure 6 contains results generated in real-time on-board a ground mobile robot equipped with a 3-D laser scanner acquiring 100,000 points per second with centimeter range resolution. The robot traversed, at two meters per second, a scene containing trees of various sizes, with few vegetated areas. The data is cropped at 3 m in elevation, as it was intended for ground mobility analysis. The figure shows tree trunks segmented, identified and modeled automatically and reliably. A mesh representing the ground surface is drawn in red and cylinders representing tree trunks and large branches are in yellow.

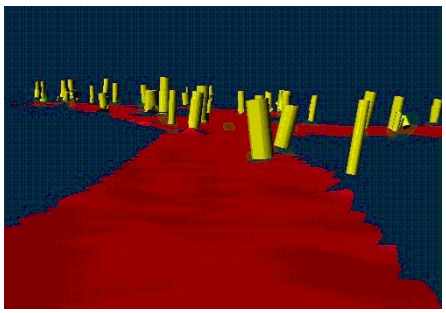

Figure 6: Results from on-board data processing, from a ground mobile robot for mobility analysis. In red, the ground surface with vegetation filtered, in yellow tree trunks segmented

3-D data is accumulated using the pose information provided by the robot navigation system which relies on inertial, odometry, and GPS measurements. Ground truth was not available for this dataset.

4.2 Static ground laser scanner data processing

A crucial feature of the proposed approach is its applicability to a variety of range sensors. The results presented are obtained from 3-D data collected with five different sensors including different measurement technologies (AM-CW [9] vs. time-of-flight [8]), and scanning patterns (1-D scans [11] vs. 2-D raster scan [8] vs. 360^o hemispheric scan [9]). For example, the left image of Figure 7 shows the segmentation results from a AM-CW laser range finder with very high resolution panoramic scanning, while the right image shows a result from a long range, low density time-of-flight scanner. Note that, in both images the tree trunk cluttered by vegetation is segmented correctly.

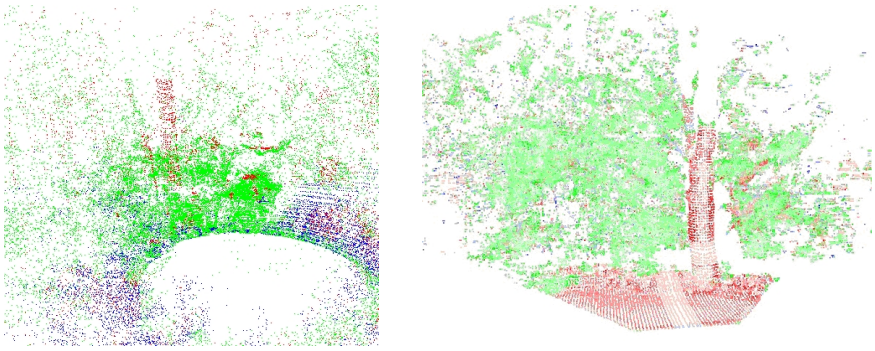

Figure 7: Examples from two others ground laser scanners. (left) From a high-density, mm resolution scanner, the Zoller-Frohlich LARA-2500. (right) From a long range scanner, the Riegl ZMS 210.

Figure 8: Laser scanners used. From left to right: actuated SICK lasers, Zoller-Frohlich laser, Riegl laser, the SIAB scanner.

4.3 Aerial data processing

The proposed technique was also applied to 3-D dense aerial data (several points per square meters, 15 cm position accuracy, cm range resolution, first echo) collected from an autonomous helicopter, for terrain classification and tree trunks detection. Such data points are much sparser and noisier than the ground data results presented so far. Figure 9 contains classification results with aerial data.

In Figure 10, we project the vertical linear structure to the recovered ground surface, spatially smooth the results and look for local maxima in the point density. Tree locations are represented by a red cylinder. Ground truth was not available for this data set.

4.4 Tree trunk diameter estimation

This section focuses on tree trunk diameter estimation at breast height (as opposed to detection). Data is collected with a relatively low cost, low density and centimeter

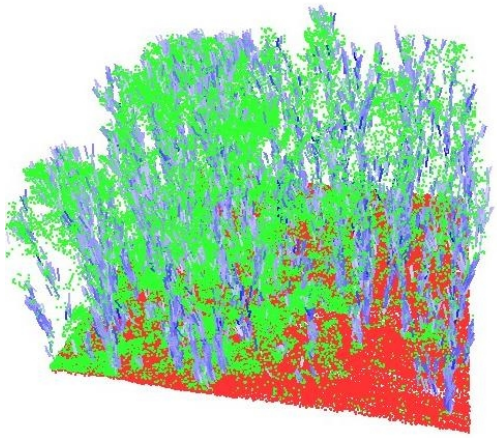

Figure 9: Extension to aerial data processing. Scene segmentation from data collected by an unmanned helicopter (Self-reference). In red, the ground surface, in green, the tree canopy and ground vegetation, in blue, branches and tree trunks

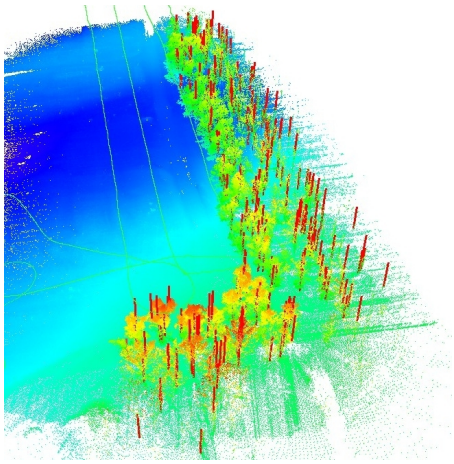

Figure 10: Tree trunks detection from overhead laser data. In red, a cylinder corresponding to the tree location, the other points are raw laser data color-coded by elevation.

range resolution static ground laser range finder. Each laser scan is made of 700×400 points separated by $\frac{2}{3} \times \frac{1}{4}$ degrees. Figure 11 contains one instance of the collected data .

The data was processed, as described in Section 3, to detect and automatically segment tree trunks and extracted the tree trunks diameter from the laser data using the 3-D cylinder fitting technique. We report here the results from three different scenes, containing 17 trees at distances ranging from 4 to 25 meters. Tree diameters range

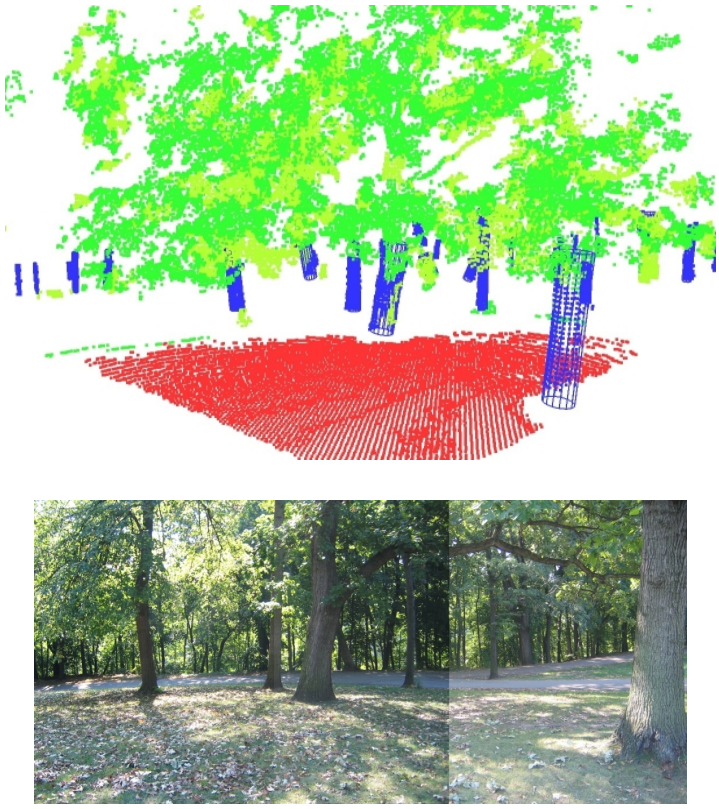

Figure 11: One of the scenes used to evaluate the performance of our approach to estimate tree trunk diameter. (Top) Segmented scene with isolated tree-trunks and fitted cylinders. (Bottom) Panoramic image of the scene.

from 30 to 70 cm. The number 3-D points per tree trunk varies between 300 and 2500. Note that this is several order of magnitude lower than the point density used in [13]. Table 1 presents the overall basic statistics from those tests.

Mean error	5 cm	11 percent
Error Standard deviation	2 cm	6 percent
Minimum Error	1 cm	3.6 percent
Maximum Error	9 cm	20 percent

Table 1: Recovered tree trunk diameter error from 17 tree trunks

Figure 12-(top) presents the distribution of diameter estimation error as a function the tree diameters and the distance to the laser. Figure 12-(bottom) shows the number of points on target for similar parameters. Note that in both cases, no cluster can be observed, probably due to the small size of our test sample.

Figure 13 presents two additional results from the SIAB laser scanner presented

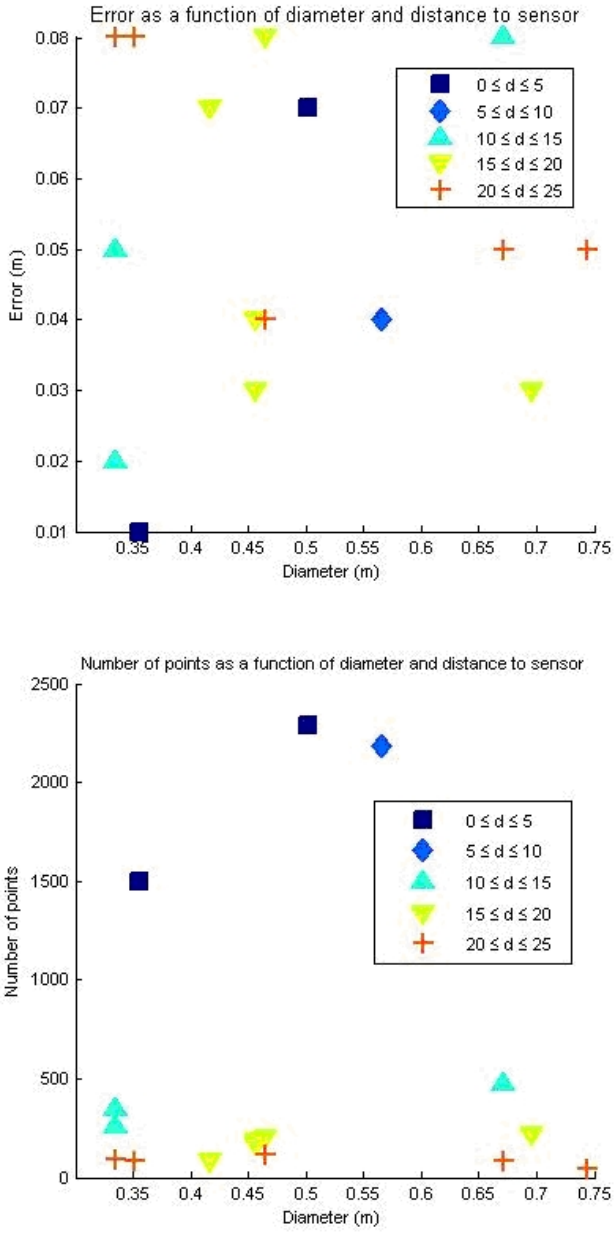

Figure 12: Distribution of the measurements. (Top) error = F(diameter, distance). (Bottom) number of points = F(diameter, distance). Different symbols indicate different range of tree-sensor distances

in Figure 8. Note how the foliage and the vegetation on the ground are segmented correctly.

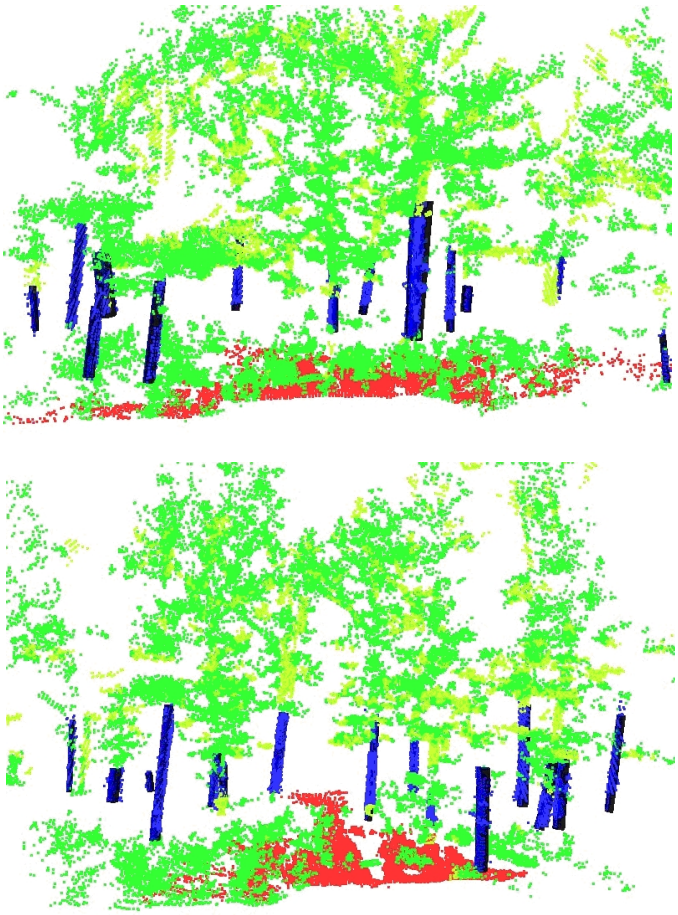

Figure 13: Example of tree trunks segmentation in another setting. Note the vegetation on the ground correctly segmented

5 Conclusion and discussion

In this paper, we present a generic approach to automatically process 3-D point cloud collected by laser scanners from natural environments. We show how this approach, though initially developed to enhance ground robot mobility, can be used to classify, segment tree trunks and recover measurements such as tree diameter at breast height.

Our approach yields many potential benefits for forest inventory in term of cost efficiency, versatility and extensibility:

- **Generic.** We developed a generic approach that can handle point clouds generated by any laser scanners, both ground and aerial based. In contrast, many approaches rely on characteristics of a specific sensor and cannot be transferred to other systems. We believe that our approach will be more cost efficient by supporting multiple systems adapted to different environments, cost constraints, and applications. Key to this flexibility is our adaptive design in which the parameters at the heart of our system are learned from actual sensor data instead of being manually engineered.
- **Low cost system**. This approach was demonstrated using a low-cost sensor can be used with data from low-cost hardware.
- **Systematic, large scale environment coverage.** Our approach has the potential to allow large scale and systematic inventory, instead of sampled inventory like described in [16]. We demonstrated on-board data processing at speed ranging from 1 to 2 m/s with a laser scanner covering a 40×40 m^2 ground area. That would correspond to a coverage of at least 35 acres per hour. It can also lead to an increase in the number of surveys performed over time to track evolution.
- **More reliable/repeatable feature extraction.** Because our approach is automatic and 3-D data driven, it will allow more reliable feature extraction, in a repeatable manner.
- **Extended features.** It will allow allow the extraction of new features that are currently out of reach of manual inventory or other approaches [16], for example 3-D foliage distribution within the canopy.
- **On the fly evaluation** Our approach allows estimation from 3-D data on-the-fly, providing a real-time analysis capability.

We are currently considering further improvements such as co-registration of overlapping scans, which would allow better reconstruction and diameter estimation from many static scans, without the need of any additional hardware. The extraction of additional information is also envisioned at the tree level and region level. For example, given sufficient visibility, tree height, bole height, 3-D structure of the canopy, foliage profile and Leaf Area Index can be estimated.

Acknowledgements

Prepared in part through collaborative participation in the Robotics Consortium sponsored by the U.S Army Research Laboratory under the Collaborative Technology Alliance Program, Cooperative Agreement DAAD19-01-209912. We would like to thank the CMU Autonomous Helicopter for providing us data.

References

[1] J. Bilmes. A gentle tutorial on the em algorithm and its application to parameter estimation for gaussian mixture and hidden markov models. Technical Report ICSI-TR-97-021,

Berkeley, CA, USA: The International Computer Science Institute, University of Berkeley, 1997.

[2] J. Byrnes and S. Singh. Precise image segmentation for forest inventory. Technical Report cmu-ri-tr-98-14, Carnegie Mellon University, Pittsburgh, PA, USA, 1998.

[3] N. Chernov and C. Lesort. Least squares fitting of circles. *Journal of Mathematical Imaging and Vision*, 23:pp. 239–251, 2005.

[4] N. Clark and S. Lee. Ground-based remote sensing with long lens video camera for upper-stem diameter and other tree crown measurement. In *Proceedings of the Tenth Forest Service Remote Sensing Applications Conference*, 2004.

[5] D. Culvenor, D. Jupp, J. Lovell, and G. Newnham. Evaluation and validation laser radar systems for native and plantation forest inventory. Technical report, Forest and Wood Products Research and Development Corporation, 2005.

[6] M. Demeyere and C. Eugene. Measurement of cylindrical objects by laser telemetry: a generalization to a randomly tilted cylinder. *IEEE Transactions on Instrumentation and Measurement*, 53(2):pp. 566 – 570, 2004.

[7] J. Juujarvi, J. Heikkonen, S. Brandt, and J. Lamninen. Digital image based tree measurement for forest inventory. In *Proceedings of SPIE, Intelligent Robots and Computer Vision XVII: Algorithms, Techniques, and Active Vision*, volume 3522, 1998.

[8] J.-F. Lalonde, N. Vandapel, D. Huber, and M. Hebert. Natural terrain classification using three-dimensional ladar data for ground robot mobility. *To appear in the Journal of Field Robotics*, 2006.

[9] D. Langer, M. Mettenleiter, F. Hartl, and C. Frohlich. Imaging ladar for 3-d surveying and cad modeling of real world environments. *International Journal of Robotics Research*, 19(11), 2000.

[10] D. Lukacs, D. Marshall, and R. Martin. Faithful least-squares fitting of spheres, cylinders, cones and tori for reliable segmentation. Technical Report 1068, Computer and Automation Research Institute, Budapest, 1997.

[11] J. Miller. *A 3D Color Terrain Modeling System for Small Autonomous Helicopters*. PhD thesis, School of Computer Science, Carnegie Mellon University, 2002.

[12] N. Pfeifer, B. Gorte, and D. Winerhalder. Automatic reconstruction of single trees from terrestrial laser scanner data. In *XXth ISPRS Congress*, 2004.

[13] N. Pfeifer and D. Winterhalder. Modelling of tree cross sections from terrestrial laser-scanning data with free-form curves. In *International Archives of Photogrammetry, Remote Sensing and Spatial Information Sciences, Volume XXXVI, Part 8/W2*, 2004.

[14] C. Schtt, T. Aschoff, D. Winterhalder, M. Thies, U. Kretschmer, and H. Spiecker. Approaches for recognition of wood quality of standing trees based on terrestrial laser-scanner data. In *Proceedings of Natscan, Laser-Scanners for Forest and Landscape Assessment - Instruments, Processing Methods and Applications. IAPRS Vol XXXVI, 8/W2*, 2004.

[15] M. Thies and H. Spiecker. Evaluation and future prospects of terrestrial laser-scanning for standardized forest inventories. In *Proceedings of the ISPRS working group VIII/2 Laser-Scanners for Forest and Landscape Assessment*, 2004.

[16] US Department of Agriculture, Forest Service. *Forest inventory and analysis national core field guide*, 2005.

[17] N. Vandapel, D. F. Huber, A. Kapuria, and M. Hebert. Natural terrain classification using 3-d ladar data. In *IEEE International Conference on Robotics and Automation*, 2004.